



Experimental Investigation on Shear Strength of Prestressed Concrete Deep Beams

A.Asran¹, H.El-Esnawi², A.Hafiz³, M.A.Eita⁴

¹Prof. Civil Engineering Dept., Faculty of Engineering, Al-Azhar University, Cairo, Egypt

²Ass.Prof. Civil Engineering Dept., Faculty of Engineering, Al-Azhar University, Cairo, Egypt

³Lecturer Civil Engineering Dept., Faculty of Engineering, Al-Azhar University, Cairo, Egypt

⁴Lecturer Assistant, Civil Engineering Dept., Higher Technological Institute 10th of Ramadan City, Egypt

الملخص

ينضمّن البحث دراسة سلوك الكمرات الخرسانية المسلحة العميقة سابقة الاجهاد بسيطة الارتكاز المعرضة لقوي قص ناتجة من تأثير حمل واحد في منتصف الكمرة وقد إستندت الدراسة علي النتائج المعملية التي تم اجراؤها علي 14 كمرة مسلحة تشتمل علي بعض المتغيرات الرئيسية التي لها التأثير الأكبر علي مقاومة الكمرات في القص وهذه المتغيرات هي : نسبه البحر الفعال الي عمق الكمره و العمق الفعال للكمره و تأثير قوي سبق الاجهاد علي مساحه مقطع الكمره و مقاومه الخرسانه. جميع الكمرات تم إختبارها حتي الانهيار وتم تسجيل القراءات والملاحظات ورصد أشكال الشروخ وحمل القص الأقصى ورسم منحنيات وذلك بغرض دراسة تأثير العوامل المختلفة علي مقاومة القص للكمرات الخرسانية العميقة المسلحة سابقه الاجهاد.

Abstract

In this paper, fourteen un-bonded post-tensioned deep beams without web reinforcement were tested under monotonically increasing single load up to failure. The investigated parameters included; the clear span to height ratio (L_n/h), the beam size h , the average pre-compression (P_e/A), and the Concrete compressive strength f'_c . Test results indicated enhancement of shear strength by the decreasing of (L_n/h), beam size increasing, (P_e/A) increasing, and increasing of f'_c .

Keywords: deep beams; diagonal tension; prestressed concrete; shear strength; Post-tensioned.

2. Introduction

The design of deep beams is a significant subject in structural engineering practice. For instance, deep beams are usually used in the design of transfer girders, shear walls, corbels, offshore structures, and pile caps. In addition, applying pre-stressing to deep beams notably enhances their flexural and shear capacities [1-3].

Despite the importance of prestressed deep beams, a limited number of experimental studies have been conducted on their shear behavior, especially, experiments on un-bonded post-tensioned deep beams. In addition, there is no agreement between the previous researchers on an integrated approach to either model the shear behavior or determine the shear strength of unbounded post-tensioned deep beams [4-9].

The aim of this paper is to experimentally investigate the effect of some parameters on the shear strength of un-bonded post-tensioned deep beams without web reinforcement. The investigated parameters are the clear span to height ratio L_n/h , the beam size h , the average pre-compression P_e/A , and the Concrete compressive strength f'_c .

3. Experimental program

In the reinforced concrete structures laboratory at Al-Azhar University, an experimental program was conducted. The experimental program included testing of fourteen reinforced concrete post tensioned deep beams subjected to shear failure.

3.1 Beam specimens

Figure 1 and table 1 show the details of the tested specimens. The tested beams were grouped in four groups. The identification of any specimen consisted of four characters, the first two characters indicated the group number, and the second two indicated the beam number in the group.

The main parameter among the first group specimens was the clear span to height ratio (L_n/h). All first group specimens had a constant height of 600 mm. and variable clear span. Thus, the clear span to height ratio (L_n/h) varied from 2.5 to 4.0. In addition, the main parameter among the specimens of second group was the beam size. Therefore, all beams had a constant span of 2200 mm. and variable height from 500 to 800 mm. Moreover, the main parameter among the specimens of the third group was the average pre-compression (P_e/A). The average pre-compression varied from 0.95 to 1.86 MPa, all other parameters were kept constant. Furthermore, the main parameter among the tested specimens of the fourth group was the concrete compressive strength (f'_c). Concrete compressive strength varied from 43.5 to 73.5 MPa.

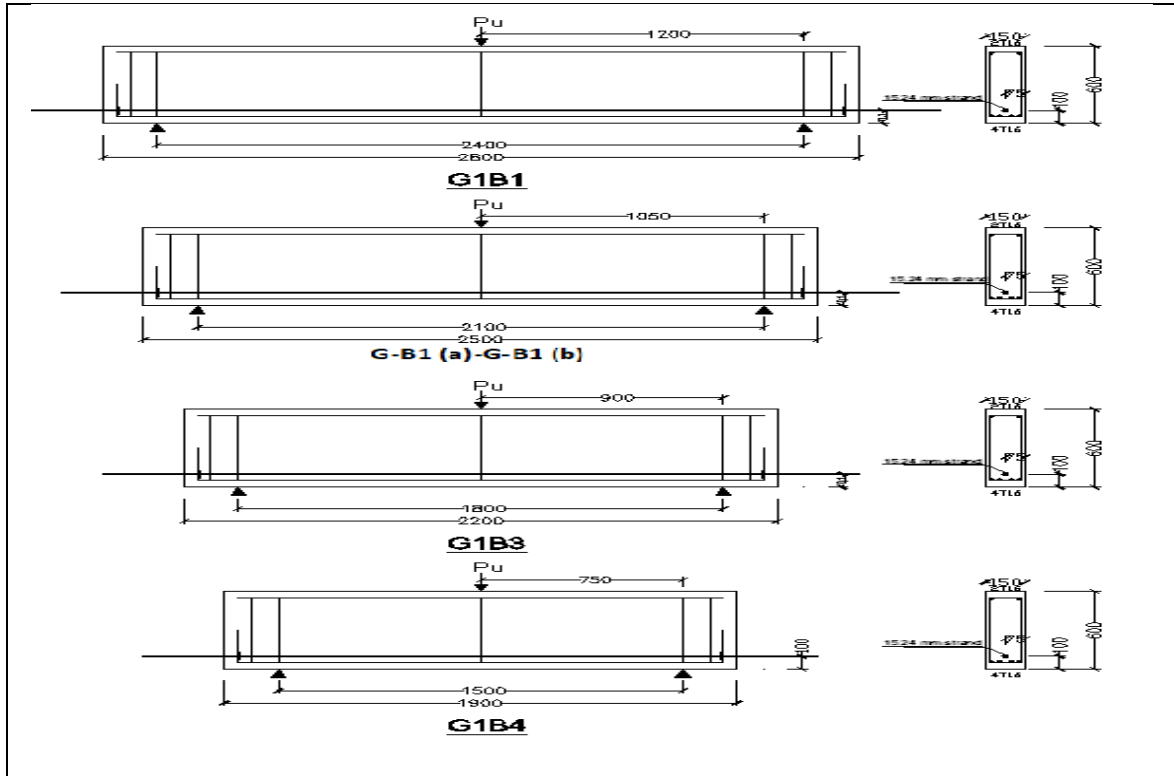
3.2 Material properties

Concrete compressive and tensile strengths of each specimen (f'_c & f_t) are included in table 1. These values were determined by the mean value of six standard cylinders (150x300mm.). Three cylinders were used to determine the average compressive strength and three were used to determine concrete tensile strength. Cylinders were casted using the same specimen concrete and tested on the same specimen-testing day.

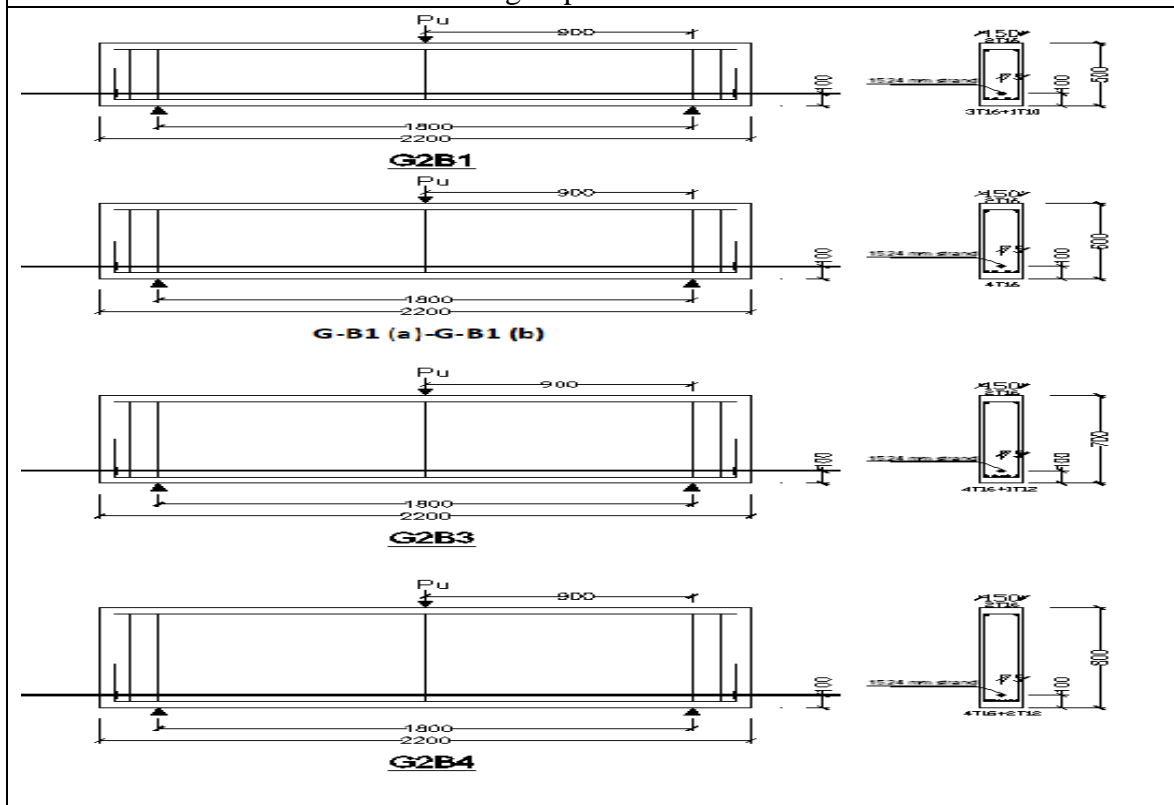
The ordinary reinforcement of the test specimens was high-grade deformed bars of 10, 12, and 16-mm. diameter. The pre-stressing reinforcement was un-bonded 15.24 mm. low relaxation seven wire mono strands. Stressing of the tested specimens was applied just before testing of the specimen. Thus, long-term losses were not taken into account. However, table 1 shows the mechanical properties of the ordinary and pre-stressing reinforcement.

3.3 Instrumentation and test setup

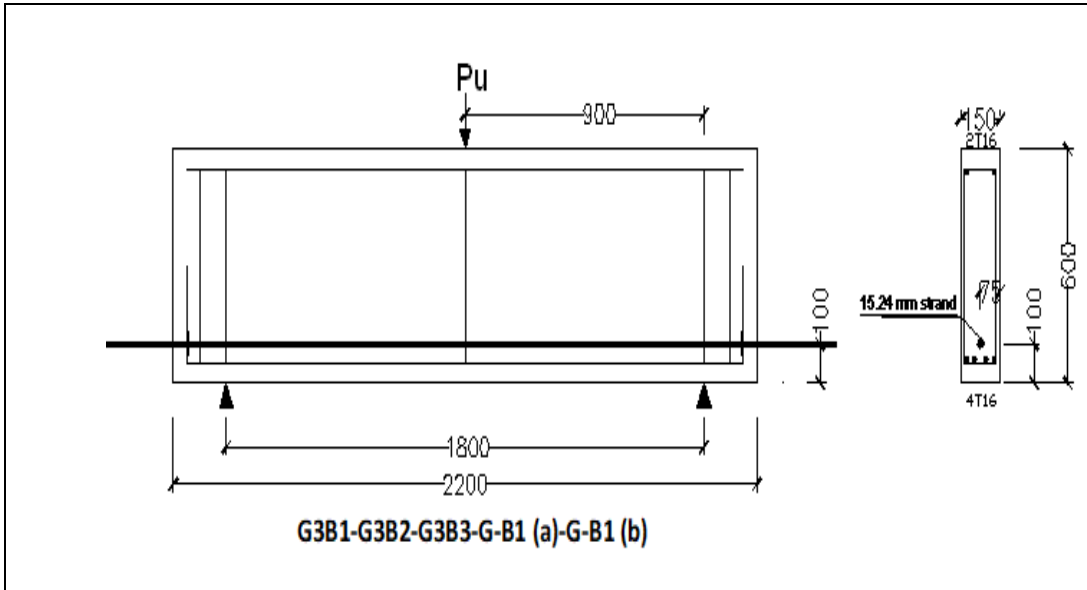
Figure 2 shows the location of the attached steel strain gauges. Strain gauges were attached on the bottom bars reinforcement in the mid span and mid shear span, respectively. In addition, Figure 3 shows the test setup. Load and mid span deflections were measured using electronic load cell and linear variable displacement transducer (LVDT), respectively. Moreover, the diagonal crack width and diagonal strain were measured using a crack width transducer and strain gauge, respectively. Instruments were attached to a data acquisition system. Thus, all data was recorded simultaneously.



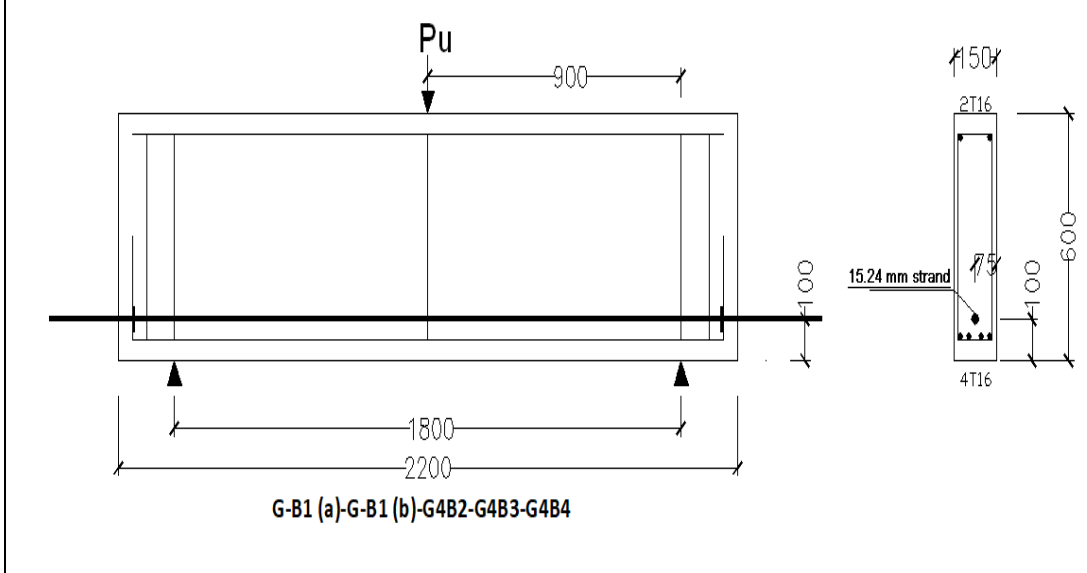
a- First group.



b- Second group.



c-Third group.



d-Forth group.

Figure 1. Details of the tested specimens.

Table 1. Details of the experimental program																	
Beam Specimen	Beam dimensions						Concrete strength		Pre-stressing data					Reinforcement			
	L mm	L_n mm	a mm	b mm	h mm	L_n/h	f'_c Mpa	f_t Mpa	A_{ps} mm ²	d_p mm	f_{pu} Mpa	P_e kN	P_e/A Mpa	f_y Mpa	A_{sb} mm ²	A_{st} mm ²	d mm
First group- Variable L_n/h																	
G1B1	2800	2400	1200	150	600	4.00	48.4	4.8	138	500	1860	86	0.95	450	804.0	402.0	550
G1B2	2500	2100	1050	150	600	3.50	45.9	4.3	138	500	1860	86	0.95	450	804.0	402.0	550
GB1(a)	2200	1800	900	150	600	3.00	43.5	4.2	138	500	1860	86	0.95	450	804.0	402.0	550
GB1(b)	2200	1800	900	150	600	3.00	46.1	4.3	138	500	1860	86	0.95	450	804.0	402.0	550
G1B4	1900	1500	750	150	600	2.50	45.1	4.4	138	500	1860	86	0.95	450	804.0	402.0	550
Second group- variable size																	
G2B1	2200	1800	900	150	500	3.60	44.4	4.3	138	400	1860	72	0.95	450	681.5	402.0	450
GB1(a)	2200	1800	900	150	600	3.00	43.5	4.2	138	500	1860	86	0.95	450	804.0	402.0	550
GB1(b)	2200	1800	900	150	600	3.00	46.1	4.3	138	500	1860	86	0.95	450	804.0	402.0	550
G2B3	2200	1800	900	150	700	2.57	45.1	4.4	138	600	1860	100	0.95	450	917.0	402.0	650
G2B4	2200	1800	900	150	800	2.25	44.3	4.29	138	700	1860	115	0.95	450	1030	402.0	750
Third group- variable average pre-compression																	
G3B1	2200	1800	900	150	600	3.00	49.1	4.7	138	500	1860	168	1.86	450	804.0	402.0	550
G3B2	2200	1800	900	150	600	3.00	46.6	4.6	138	500	1860	132	1.46	450	804.0	402.0	550
G3B3	2200	1800	900	150	600	3.00	52.4	4.9	138	500	1860	109	1.21	450	804.0	402.0	550
GB1(a)	2200	1800	900	150	600	3.00	43.5	4.2	138	500	1860	86	0.95	450	804.0	402.0	550
GB1(b)	2200	1800	900	150	600	3.00	46.1	4.3	138	500	1860	86	0.95	450	804.0	402.0	550
Forth group- variable concrete compressive strength																	
GB1(a)	2200	1800	900	150	600	3.00	43.5	4.2	138	500	1860	86	0.95	450	804.0	402.0	550
GB1(b)	2200	1800	900	150	600	3.00	46.1	4.3	138	500	1860	86	0.95	450	804.0	402.0	550
G4B2	2200	1800	900	150	600	3.00	56.6	5.3	138	500	1860	86	0.95	450	804.0	402.0	550
G4B3	2200	1800	900	150	600	3.00	64.3	5.9	138	500	1860	86	0.95	450	804.0	402.0	550
G4B4	2200	1800	900	150	600	3.00	73.3	6.7	138	500	1860	86	0.95	450	804.0	402.0	550

L, beam span; L_n , clear beam span; a, shear span; b, beam width; h, beam height; f'_c and f_t , compressive and tensile concrete strength, respectively; A_{ps} , area of strand; P_e , effective pre-stressing force; d_p , depth to pre-stressing strand, A_{sb} and A_{st} , bottom and top reinforcement area, respectively; d, depth to ordinary reinforcement. Note: (G-B1(a), G-B1(b)) having same the same dimensions and characteristics, these are common to all groups.

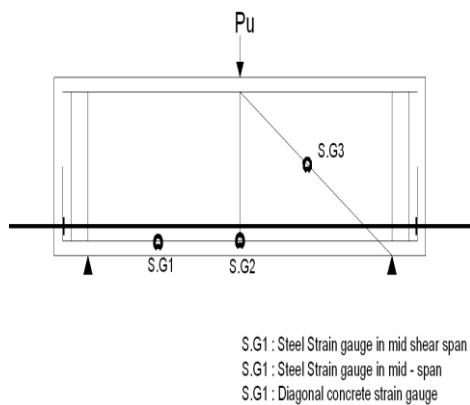
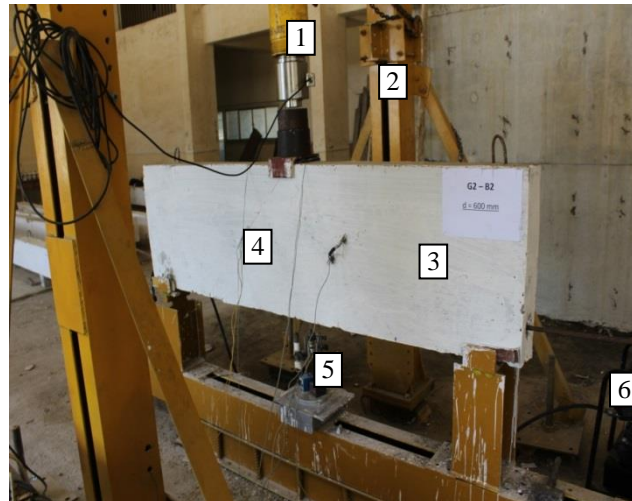


Figure 2. Strain gauges locations.



1. Hydraulic jack.
2. Load cell.
3. Crack width transducer
4. Diagonal strain gauge.
5. LVDT.
6. 15.24mm strand.

Figure 3. Test setup.

4. Test results and discussion

4.1 Cracks and failure mode.

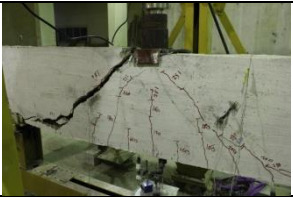













Figure 4 shows the crack pattern at failure for the tested specimens. For all specimens, first crack was flexural crack at the mid span region. With further load increase, diagonal cracks initiated and extended toward the supports and the beam compression zone. Consequently, with further load increase, the diagonal cracks width and the cracks intensity increased. At the ultimate load, beams failed with different failure modes. The failure modes of all test specimens are also included in figure 4. Failure modes of the tested specimens varied between diagonal splitting (the splitting plan connecting the inner side of the loading plate with the inner side of the support plate), diagonal crushing, and diagonal crushing combined with upper node crushing, diagonal splitting with crushing of upper node, and bearing failure under the loading plate.

4.1.1 Effect of clear span to height ratio (L_n/h)

With the decrease of the clear span to height ratio (L_n/h), the cracks intensity increased, the cracks inclination angle became steeper, and the failure mode shifted from diagonal splitting to crushing of concrete diagonal struts. With the decrease of the clear span, the load transferred via arch action rather than beam action, and the cracks intensity width increased at relatively higher load levels.

4.1.2 Effect of beam size

The increase in the beam height led to an increase in the cracks intensity, the cracks inclination angle became steeper as the beam height increased. Further increase in the diagonal strut length led to a change in the failure mode from crushing of concrete strut to bearing failure at the top node for specimen G2B4.

Beam	G1B1	G1B2	G1B4
Failure pattern			
Failure mode	Diagonal splitting	Diagonal splitting with upper node crushing	Diagonal crushing with upper node crushing
Beam	G2B1	G2B3	G2B4
Failure pattern			
Failure mode	Diagonal splitting with down node crushing	Diagonal crushing	Bearing failure under loading plate
Beam	G3B1	G3B2	G3B3
Failure pattern			
Failure mode	Diagonal crushing with down node crushing	Diagonal crushing with upper node crushing	Diagonal splitting with upper node crushing
Beam	G4B2	G4B3	G4B4
Failure pattern			
Failure mode	Diagonal splitting	Diagonal splitting	Diagonal splitting
	G-B1(a)	G-B1(b)	
			Figure 4. Crack pattern.
	Diagonal splitting	Diagonal splitting with upper node crushing	

4.1.3 Effect of average pre compression (P_e/A)

Increasing the pre-stressing force decreased the cracks intensity, but did not affect the flexural first crack load. Alternatively, the increase of the prestressing force increased the diagonal crack load. In addition, the increase of the pre-stressing force changed the failure mode from diagonal splitting to crushing of the diagonal strut combined with crushing of the beam upper node.

4.1.4 Effect of concrete compressive strength (f'_c)

The number of cracks and cracks widths decreased with the increase of the concrete compressive strength, this was combined with significant increase in the diagonal crack load.

4.2 Load verses mid span deflection

Figure 5 shows the load verses mid span deflection relationships for the tested specimens. The first cracking load, the diagonal cracking load, and the yield of the flexural reinforcement are also assigned on the curves.

4.2.1 Effect of clear span to height ratio (L_n/h)

The ultimate load increased with the decrease of the span to height ratio (L_n/h). In addition, the initial stiffness of all specimens was not affected either by the first flexural crack or by the first diagonal crack.

The domination of the arch action on the behavior of the specimens was evident with the increase of the clear span to height ratio (L_n/h) of more than 2.5. For instance, specimen G1B1 exhibited pre mature shear failure prior yield of tension reinforcement; thus, the tension tie in the arch-tie mechanism of the beam specimen was not fully utilized. The beam action is more likely to represent the behavior of G1B1.

On the contrary, for the rest of the specimens of the first group, tension reinforcement exhibited yield in the mid beam span and mid shear span prior shear failure. The load values corresponding to yield in mid span and mid shear span were close. Therefore, tension tie was fully utilized, tension tie stresses were almost uniformly distributed along bars length, and the strength of the arch-tie action mechanism controlled the shear capacity of the specimens.

4.2.2 Effect of beam size

For the specimens of the second group, the ultimate load increased with the increase of the beam size. In addition, all beams (except G2B4) exhibited strength degradation consequent to yield of tension reinforcement. For specimen G2B4 ($h=800\text{mm}$.), local bearing failure occurred below the loading plate (in the upper nodal zone). This was regarded to relatively big diagonal strut size and inappropriate loading plate size. However, failure of G2B4 occurred prior any yielding of tension reinforcement.

4.2.3 Effect of average pre-compression (P_e/A)

Increasing the average pre-compression increased the ultimate load of the tested specimens significantly. In addition, increasing the average pre-compression pushed the tie tensile stresses concentration toward beam mid span. This observation was obvious by comparing the behavior of specimen G3B1 ($P_e/A = 1.86$) with specimen GB1 (a) and GB1 (b) ($P_e/A = 0.95$). For specimens GB1 (a) and GB1 (b) yield in mid span and mid shear span occurred almost simultaneously indicating uniform tie tensile stress distribution. On the other hand, for specimen G3B1, yield in the mid span preceded yield in the mid shear span, the difference between the two yields loads was about 20%.

Nevertheless, the beam was able to sustain increasing load even after beam flexural stiffness degradation.

However, beams with relatively high average pre-compression ($P_e/A > 1.21$) were able to sustain excessive deformations and extensive strains prior shear failure. For beam G3B3 ($P_e/A = 1.21$) balanced flexural failure occurred with shear failure; i.e. yield in bottom reinforcement occurred in combination with compression zone crushing and diagonal splitting.

4.2.4 Effect of concrete strength f'_c

The beams ultimate load was increased with the increase of the concrete compressive strength. This increase was combined with decrease in the maximum deflection at failure.

4.3 Shear strength of tested beams

Figure 6 shows the shear strength against different parameters relationships for the tested specimens. To make this comparison, normalization had been made by dividing $V_u/bd\sqrt{f'_c}$ in the first three group.

4.3.1 Effect of clear span to height ratio (L_n/h)

The increase of clear span to height ratio (L_n/h) decreased the shear strength. The decrease of shear strength was more obviously with the increase of (L_n/h) from 2.5 to 3.0. Increase of (L_n/h) more than 3.0 the shear strength decrease with less significant.

4.3.2 Effect of beam size

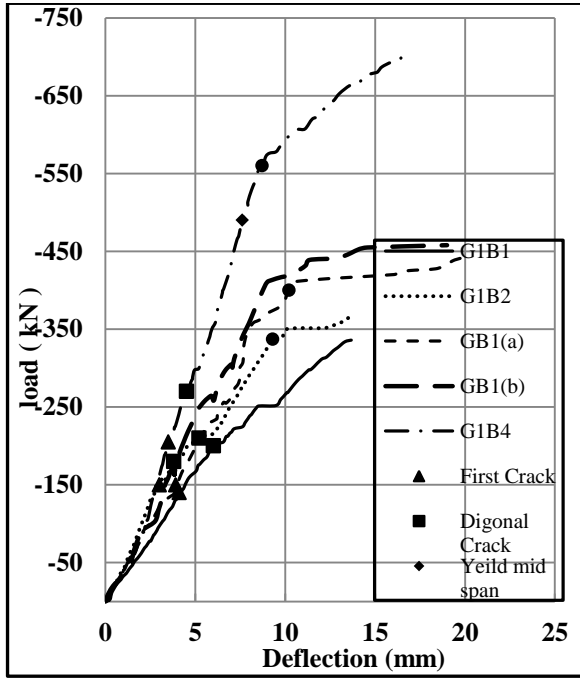
For all beams (except G2B4) the shear strength increased with increase of beam size. This was regarded to for specimen G2B4 ($h=800\text{mm.}$), local bearing failure occurred below the loading plate (in the upper nodal zone).

4.3.3 Effect of average pre-compression (P_e/A)

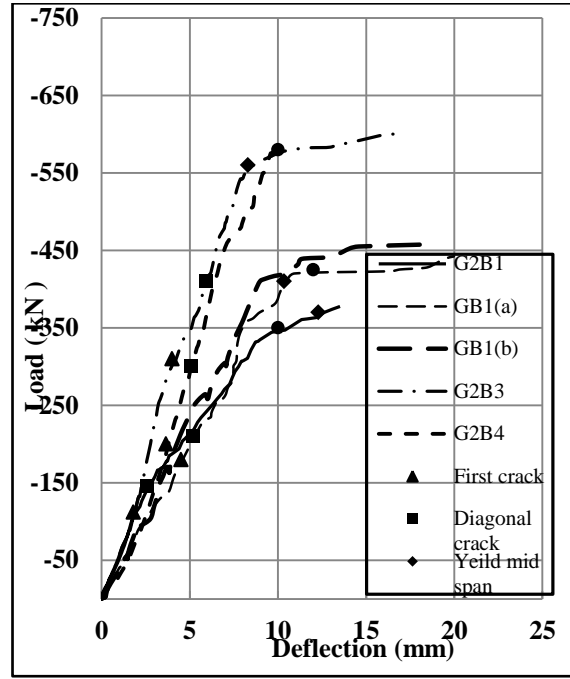
Increasing the average pre-compression (P_e/A) from (1.21) to (1.46) increase the shear strength of the tested specimens significantly. Decreasing (P_e/A) less than (1.21) or increasing (P_e/A) more than (1.46) does not affect the shear strength.

4.3.4 Effect of concrete strength f'_c

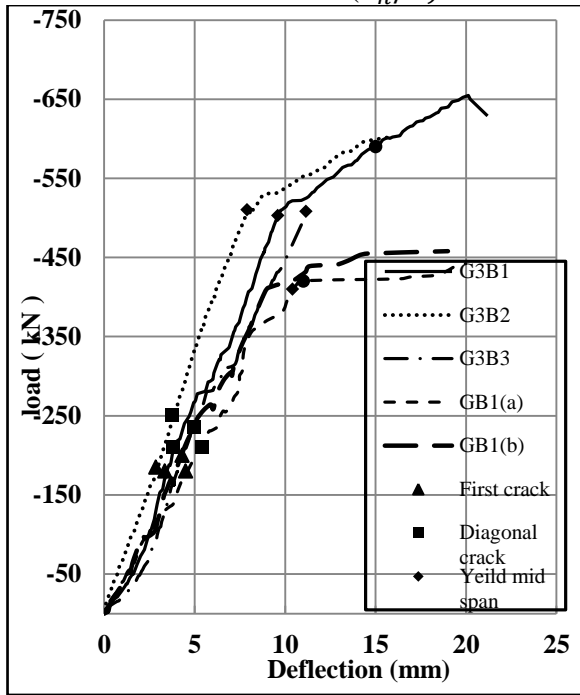
The beams shear strength was increased with the increase of the concrete compressive strength.



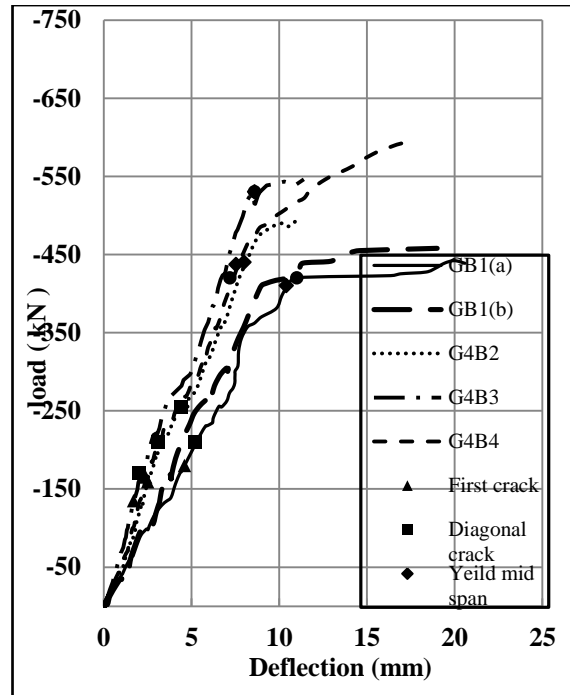
a- Effect of (L_n/h)



b- Effect of beam size



c- Effect of (P_e/A)



d- Effect of (f'_c)

Figure 5 The load versus mid span deflection relationship for the tested specimens

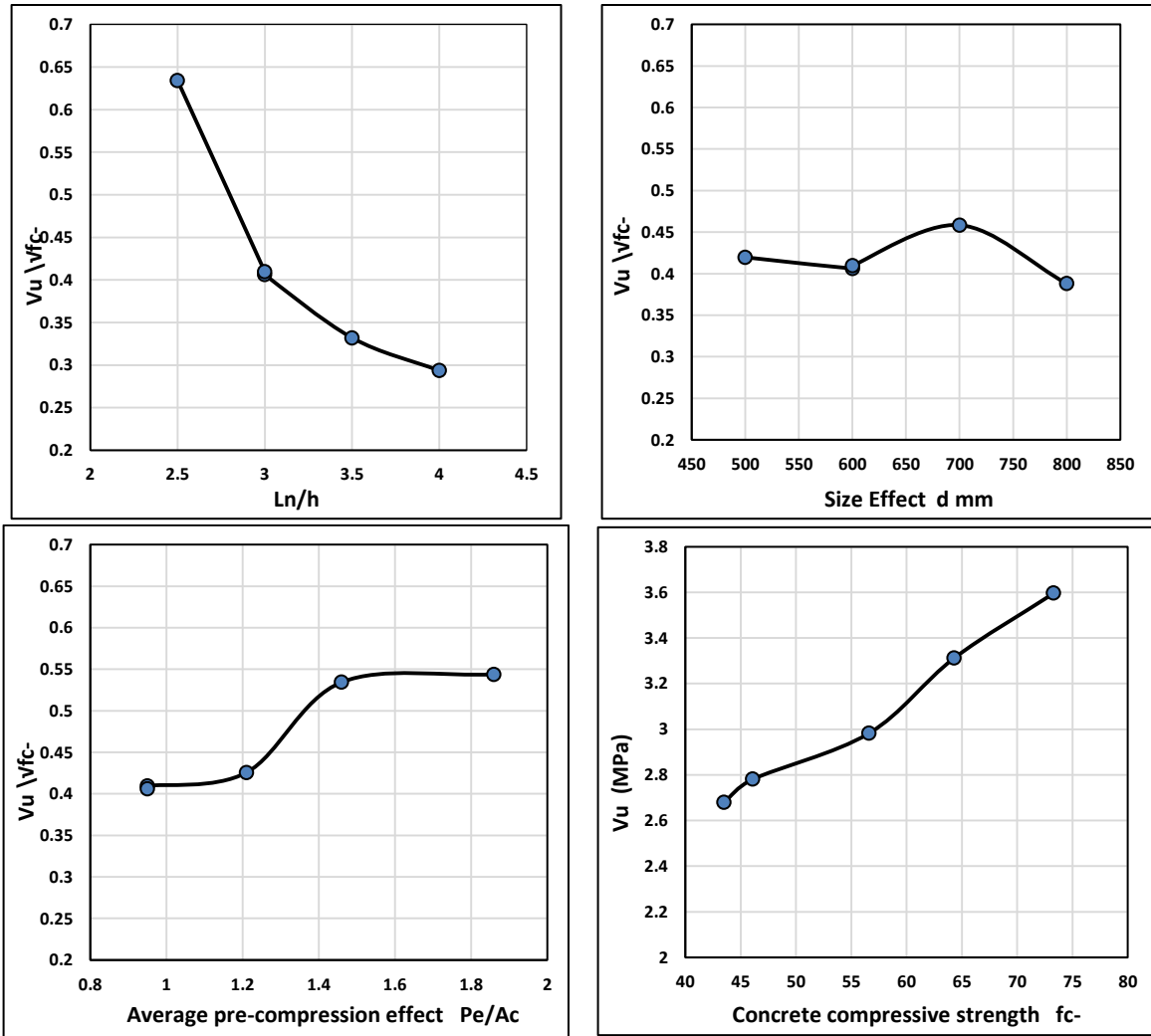


Figure 6 shear strength of tested beams

6.0 Conclusions

- The domination of the arch action on the behavior of the specimens was evident with the increase of the clear span to height ratio (L_n/h) of more than 2.5. In addition, the failure mode shifted from diagonal splitting to crushing of concrete diagonal struts.
- Increasing the pre-stressing force decreased the cracks intensity and changed the failure mode from diagonal splitting to crushing of the diagonal strut combined with crushing of the beam upper node.
- Decreasing the clear span to height ratio (L_n/h) from 4.0 to 2.5 increased the beams ultimate shear strength. The percentage of increase varied from 10.6% to 58.5%.
- The ultimate shear strength increased with the increase of the beam size from 500 mm. to 800 mm. The percentage of increase varied from 17.2% to 57%.
- Increasing the average pre-compression (P_e/A) from (1.21) to (1.46) increase the shear strength of the tested specimens significantly. There no significant effect beyond these limits.
- The increase of the concrete compressive strength beam was increased ultimate shear strength, this increasing about 10%.

Notations

a Shear span of deep beam
 A_s, A_{ps} Areas of unstressed and prestressed steel, respectively
 b, d, h Width, overall depth and height of deep beam, respectively
 f'_c Concrete cylinder strength
 f_{cu} Concrete cube strength
 f_{ps} Stress in prestressing steel when the beam fails
 f_{pe} effective Stress in pre-stressing steel
 f_{py} yield Strength of 7 wire strand
 f_t Tensile splitting strength of concrete
 f_y Yield strength of web reinforcement or unstressed steel
 V_n Nominal shear strength
 V_{exp} Measured ultimate shear strength.

References;

1. KONG F. K. (Ed.). Reinforced Concrete Deep Beams. Blackie and Son, London, 1990.
2. AMERICAN CONCRETE INSTITUTE COMMITTEE 318.14 Building Code Requirements for Structural Concrete. ACI, Detroit, 2014.
3. ALSHEGEIR A. and RAMIREZ J. A. Strut-tie approach in pre-tensioned deep beams. ACI Structural Journal, 1992, 89, 296–304.
4. TAN K. H. and MANSUR M. A. Partial pre-stressing in concrete corbels and deep beams. ACI Structural Journal, 1992, 89, 251–262.
5. K. H. Tan and K. Tong, Shear behavior and analysis of partially prestressed I-girders. The Structural Engineer Volume, December 1999, 77, pp.28-34.
6. Tan K. H., and Lu, H. Y., Size Effect in Large Prestressed Concrete Deep Beams, ACI Structural Journal, Nov-Dec. 1999, V. 96, No. 6, pp. 937-947.
7. Guo-Lin Wang, Shao-Ping Meng. Modified strut-and-tie model for prestressed concrete deep beams. Engineering Structures, 2008, 30, 3489-3496.
8. TENG S., KONG F. K. and POH S. P. Shear strength of reinforced and prestressed concrete deep beams. Part II: the supporting evidence. Structures and Buildings, 1998, 128, No. 2, 124–143.
9. Stephan J. Foster and R. Ian Gillbert, Experimental studies on high strength concrete deep beams, ACI STRUCTURAL JOURNAL, Vol.95, No.4, 1998. Pp.382-390.